

in the ion damaged layer is consistent with the observed maximum concentration changes upon ion bombardment. The relative insensitivity of the *total atomic concentrations* of the damaged layer to the method of energy deposition and the energy density indicates that only low energy densities are required to induce decomposition and that the level of energy deposition from all three sources exceeds this requirement. The energy in excess of this requirement drives the reactions further toward completion (e.g. the ion beam produces the largest amount of oxide and nitrite species) and is, therefore, important in determining the relative *concentrations of the specific products*.

Conclusions

Electron, X-ray, and ion irradiation of alkali metal nitrates result in preferential loss of nitrogen and formation of a damaged layer characterized by M_2O and M_2O_2 with smaller amounts of

MNO_3 and MNO_2 species. The atomic concentrations within this layer are similar for the three radiation sources, although the relative concentrations of the specific product compounds vary. Considerations of the rate of energy deposition indicate that the energy density deposited by all three sources is greater than that required for decomposition (hence the similar atomic concentrations), and that the excess energy determines the extent of reaction (hence the dissimilar concentrations of specific products).

Acknowledgment. This material is based upon work supported by the National Science Foundation under Grant No. DMR-8304658 and the Robert A. Welch Foundation under Grant No. E-656. The photoelectron spectrometer was provided by National Science Foundation Grant No. CHE-8306122.

Registry No. $LiNO_3$, 7790-69-4; $NaNO_3$, 7631-99-4; NH_4NO_3 , 6484-52-2; Li_2O_2 , 12031-80-0; Li_2O , 12057-24-8.

A High-Temperature Fast-Flow-Reactor Kinetics Study of the Reaction $AlO + CO_2 \rightarrow AlO_2 + CO$. Thermochemical Implications

Donald F. Rogowski, Andrew J. English,[†] and Arthur Fontijn*

Department of Chemical Engineering and Environmental Engineering, Rensselaer Polytechnic Institute, Troy, New York 12180-3590 (Received: August 19, 1985)

The title reaction has been studied in a high-temperature fast-flow reactor (HTFFR) at temperatures from 500 to 1300 K. Laser-induced fluorescence was used to monitor relative $[AlO]$. $k(T)$ was determined to be $(2.5 \pm 1.3) \times 10^{-14} \exp[(400 \pm 280)/T] \text{ cm}^3 \text{ molecule}^{-1} \text{ s}^{-1}$ (confidence level > 95%). The reaction probably proceeds via an intermediate complex which preferentially dissociates to the reactants. The negative activation energy implies $D(O-AlO) \geq D(O-CO) = 127 \text{ kcal mol}^{-1}$, which is incompatible with the $O-AlO$ dissociation energy obtained for AlO_2 from Al_2O_3 evaporation-mass spectrometry studies. It is argued that the latter AlO_2 may have a different structure from that of the present work.

Introduction

The development and use of the HTFFR technique¹ is leading to an experimental data base of homogeneous gas-phase oxidation reactions of refractory species. Measurements of rate coefficients $k(T)$ in the 300–1900 K range have been reported and the results have been summarized in several reviews.^{2,3} A variety of $k(T)$ dependences have been observed, including normal Arrhenius $k(T) = A \exp(-E_A/RT)$ behavior, temperature-independent rate coefficients, and reactions with a slight negative activation energy. In addition, reactions have been found the rates of which are determined primarily by the thermal equilibrium populations of excited states of the reactants. One of the most interesting results obtained so far is that for the reaction



The Arrhenius plot for this reaction shows very strong upward curvature above 700 K, well in excess of that explainable by transition-state theory for a single reaction channel.⁴ This behavior may be explained by the thermal equilibrium increase in the concentration of CO_2 in bending vibrational modes.^{2,4} To obtain substantial upward curvature in Arrhenius plots by vibrational excitation, it is necessary that the excitation leads primarily to an increase in the A factor, since a reduction in E_A by the vibrational energy is partly or exactly cancelled by the Boltzmann equilibrium increase of the population of the excited species.^{2,5} While ground-state linear CO_2 has a negative electron

affinity and hence can interact with Al only by a covalent mechanism (neutral potential surface), CO_2 in bending modes has a positive electron affinity and can interact at larger distances by an ionic (electron jump or harpooning) mechanism.^{4,6} Larger interaction distances are equivalent to larger collision cross sections and hence can lead to larger A factors.

Ionic interaction distances are roughly proportional to $[IP(\text{metallic species}) - EA(\text{oxidant})]^{-1}$, where IP is the ionization potential and EA is the electron affinity.⁷ Since generally $IP \gg EA$, ionic interactions will lead to substantially larger interaction distances only for low ionization potential reactants such as free metal atoms, e.g. $IP(Al) = 5.98 \text{ eV}$.⁸ By contrast the metal oxide, AlO has an $IP = 9.5 \pm 0.5 \text{ eV}$.⁹ As a test for the ex-

(1) (a) Fontijn, A.; Kurzius, S. C.; Houghton, J. J. *Symp. (Int.) Combust., [Proc.]*, 14th 1973, 167. (b) Fontijn, A.; Kurzius, S. C. *Chem. Phys. Lett.* 1972, 13, 507.

(2) Fontijn, A.; Zellner, R. *Reactions of Small Transient Species, Kinetics and Energetics*, Fontijn, A., Clyne, M. A. A., Eds.; Academic Press: London, 1983; Chapter 1.

(3) Fontijn, A.; Felder, W. *Reactive Intermediates in the Gas Phase. Generation and Monitoring*, Setser, D. W., Ed.; Academic Press: New York, 1979; Chapter 2.

(4) Fontijn, A.; Felder, W. *J. Chem. Phys.* 1977, 67, 1561.

(5) Zellner, R. *J. Phys. Chem.* 1979, 83, 18.

(6) (a) Bardsley, J. N. *J. Chem. Phys.* 1969, 51, 3384. (b) Cooper, C. D.; Compton, R. N. *Chem. Phys. Lett.* 1972, 14, 29. For a discussion of the analogous case of reactions of the isoelectronic molecule N_2O , see (c) Chantry, P. J. *J. Chem. Phys.* 51, 1969, 3369, 3380. (d) Wren, D. J.; Menzinger, M. *Faraday Discuss. Chem. Soc.* 1979, 67, 97. *J. Chem. Phys.* 1975, 63, 4557.

(7) Gole, J. L.; Preuss, D. R. *J. Chem. Phys.* 1977, 66, 3000.

(8) *JANAF Thermochemical Tables*, Dow Chemical Co.: Midland, MI, frequently updated.

[†] Present address: New York State Department of Environmental Conservation, Albany, NY 12233.

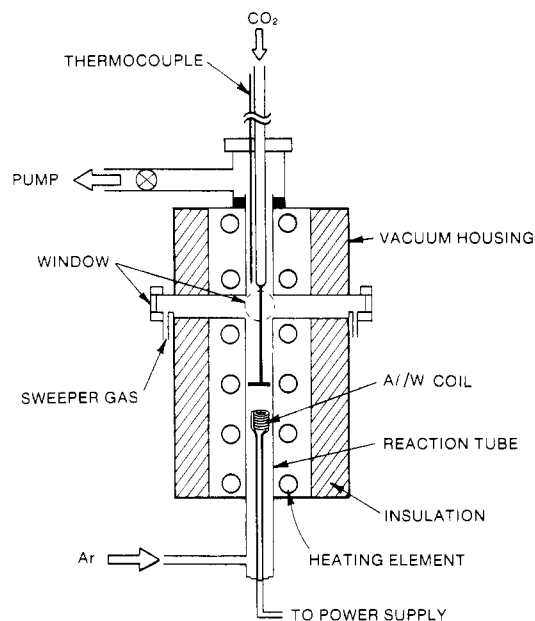
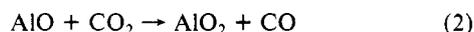


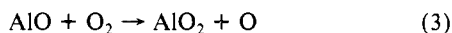
Figure 1. Schematic of reactor 2.

planation of the behavior of reaction 1 a study was undertaken of



for which no strong upward curvature, such as that observed for reaction 1, was thus anticipated.

Another reason why reaction 2 is of interest follows from the observation that



has a slight negative activation energy.¹⁰ This implies that the new bond formed is at least as strong as the O–O bond, 118 kcal mol⁻¹. This value is in apparent disagreement with the value of 100 ± 9 kcal mol⁻¹ derived from the $\Delta H_a^\circ_{298}(\text{AlO}_2)$ of Ho and Burns,¹¹ who recently observed the long-elusive AlO₂ molecule in Al₂O₃ evaporation experiments with mass spectrometer detection. Since the O–CO bond of 127 kcal mol⁻¹ is stronger than the O–O bond the activation energy of reaction 2 could supply further information on the O–(AlO) bond energy.

Technique

The experiments were performed in two newly designed single-unit HTFFRs. The basic HTFFR design has been described previously.³ In the present study 2.2-cm-i.d. 998 grade alumina reaction tubes were used. The Pt/Rh resistance heating wire used in earlier works³ was replaced by clamshell heating elements wound with Fe/Cr/Al alloy wire (Thermcraft, Inc.) in reactor 1 and, as shown in Figure 1, by silicon carbide rods (I²R Corp.) in reactor 2. Reactor 1 could be used up to about 1400 K, while the temperature limit for reactor 2 is about 1900 K. Relative Al concentration, $[\text{Al}]_{\text{rel}}$, was measured by atomic absorption,³ while $[\text{AlO}]_{\text{rel}}$ was monitored by laser-induced fluorescence (LIF).¹² For LIF a Lambda Physik EMG 101 excimer/FL 2002 dye laser combination was used to pump AlO at 464.3 nm using Exciton LD 466 dye. The AlO fluorescence was observed at 485 nm through a 490 ± 10 nm (fwhm) interference filter with an EMI 9813 QA photomultiplier tube and recorded with a Data Precision Analogic 6000/620 100-MHz transient digitizer. To smooth out the effect of fluctuations in fluorescence intensity due to variations

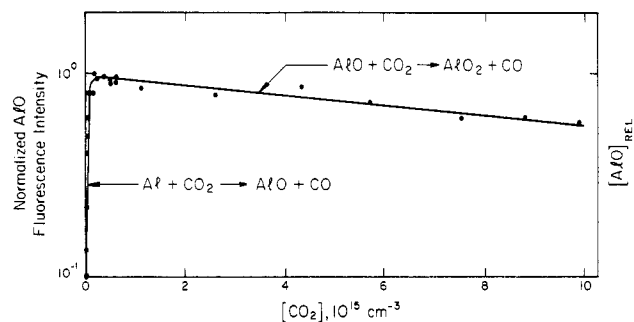


Figure 2. AlO concentration profile vs. $[\text{CO}_2]$ at a 20-cm CO_2 inlet-to-observation port distance. $P = 10.5$ torr, $\bar{v} = 112$ m s⁻¹, $T = 1190$ K.

in the laser pulse energy, the recorded fluorescence was the average of 100 pulses.

Pressure was measured downstream of the reaction tube with an MKS Baratron gauge. Measurements of the reaction zone gas temperature were obtained with a movable type R thermocouple (Pt vs. Pt/13% Rh). Temperature measurements were taken both before and after a set of kinetic measurements. The pressure and temperature measurements were corrected as discussed by Fontijn and Felder.^{3,13} Ar obtained from high-purity (99.998% min) liquid Ar was used as the bath gas. About 1% of the Ar was introduced with the CO_2 through the CO_2 inlet, the remainder, as shown in Figure 1, from the upstream side of the reactor. The oxidant gas CO_2 was obtained from 99.5% minimum liquid CO_2 . Al was vaporized from Al-wetted tungsten coils.³ Initial experiments showed that above 500 K the AlO formation reaction 1 was much faster than the AlO consumption reaction 2. This allowed driving reaction 1 to completion near the CO_2 inlet when the high $[\text{CO}_2]$ needed to observe reaction 2 was used, cf. Figure 2. The highest $[\text{CO}_2]$ used were on the order of 10 to 20% of the $[\text{Ar}]$. The flow disturbance from the correspondingly large CO_2 flows was found to be minimal, since equal flows of Ar substituted for the CO_2 produced no significant change in the observed AlO fluorescence.

Rate coefficients were measured in the stationary oxidant inlet mode at CO_2 inlet to observation window distances of 10 and 20 cm, following the procedures described previously.³ Plots of $\ln [\text{AlO}]_{\text{rel}} = \ln ([\text{AlO}]/[\text{AlO}]_{\text{max}})$, where $[\text{AlO}]_{\text{max}}$ denotes the maximum AlO concentration, vs. $[\text{CO}_2]$ yielded straight lines with slope $k_2 t$, where t is reaction time. $[\text{AlO}]_{\text{max}}$ was estimated to be on the order of 10^{10} cm⁻³. A weighted linear regression and propagation of error treatment, as described by Fontijn and Felder,^{3,13} was used to determine $k_2 t$ and in turn k_2 . In this treatment the uncertainties in $[\text{AlO}]_{\text{rel}}$ and $[\text{CO}_2]$ are combined vectorially, which allows $[\text{CO}_2]$ to be treated as if no uncertainty is associated with it. The linear regression of k_2 as a function of temperature followed the procedure of Cvetanovic et al.¹⁴ for an Arrhenius-type dependence with no error in T .

As a consistency check on the new reactors and data generation equipment, a few measurements of k_1 in the 850–1000 K regime were made. The values obtained are in excellent agreement with those of the earlier HTFFR work.⁴

Results and Discussion

Measurements of k_2 were made between 500 and 1300 K. The lower temperature was chosen because the AlO production via reaction 1 is too slow below this limit. The upper limit corresponds to the onset of major interference by thermal radiation from the reactor walls with the fluorescence measurements at the wavelength which had to be used for AlO observation. While it might have been possible to work at higher temperatures with reactor 2, the trend in $k_2(T)$ vs. T is well established by the present temperature range.

(9) Huber, K. P.; Herzberg, G. *Molecular Spectra and Molecular Structure. IV. Constants of Diatomic Molecules*, Van Nostrand-Reinhold: New York, 1974; p 28.

(10) Fontijn, A.; Felder, W.; Houghton, J. J. *Symp. (Int.) Combust., [Proc.]*, 16th 1977, 871.

(11) Ho, P.; Burns, R. P. *High Temp. Sci.* 1980, 12, 31.

(12) Fontijn, A. *Progr. Astronaut. Aeronaut.* 1984, 92, 147.

(13) Fontijn, A.; Felder, W. *J. Phys. Chem.* 1979, 83, 24.

(14) Cvetanovic, R. J.; Singleton, D. L.; Paraskevopoulos, G. *J. Phys. Chem.* 1979, 83, 50.

TABLE I: Summary of $\text{AlO} + \text{CO}_2 \rightarrow \text{AlO}_2 + \text{CO}$ Rate Coefficient Measurements^a

oxidant inlet position, cm	\bar{P} , torr	$[\bar{M}]$, 10^{17} cm^{-3}	\bar{v} , m s^{-1}	\bar{T} , K	$k \pm \sigma$, $10^{-14} \text{ cm}^3 \text{ molecule}^{-1} \text{ s}^{-1}$	oxidant inlet position, cm	\bar{P} , torr	$[\bar{M}]$, 10^{17} cm^{-3}	\bar{v} , m s^{-1}	\bar{T} , K	$k \pm \sigma$, $10^{-14} \text{ cm}^3 \text{ molecule}^{-1} \text{ s}^{-1}$
20	12.0	1.04	99	1115	3.25 ± 0.37	20	13.4	1.02	90	1268	1.79 ± 0.40
20	12.0	1.04	99	1113	2.84 ± 0.51	20	13.4	1.02	112	1265	2.87 ± 0.50
20	11.9	1.03	101	1116	5.14 ± 1.75	20	13.4	1.02	112	1265	1.83 ± 0.29
20	11.9	1.03	101	1116	3.31 ± 0.79	20	22.2	1.69	68	1266	1.54 ± 0.33
20	11.8	1.02	101	1118	3.60 ± 0.62	20	22.1	1.69	68	1266	1.63 ± 0.37
20	16.7	1.44	110	1118	3.51 ± 0.64	10	14.8	1.15	100	1247	5.24 ± 0.73
20	11.1	0.96	164	1120	7.14 ± 0.86	10	14.9	1.15	100	1247	5.57 ± 0.64
20	16.1	1.39	113	1119	2.40 ± 0.40	10	23.3	1.80	64	1246	3.86 ± 0.35
20	20.3	1.75	90	1119	1.72 ± 0.48	10	23.1	1.79	64	1246	3.91 ± 0.79
10	18.7	1.64	96	1103	3.49 ± 0.77	10	11.8	0.91	101	1246	2.33 ± 0.44
10	12.9	1.13	139	1101	9.47 ± 1.64	10	11.8	0.91	101	1246	2.98 ± 0.59
10	12.9	1.13	139	1101	6.78 ± 0.63	20	11.6	1.88	54	598	4.90 ± 0.51
10	21.4	1.87	84	1103	5.58 ± 0.78	20	11.5	1.86	54	598	5.12 ± 0.58
10	12.8	1.13	92	1100	5.75 ± 1.01	20	13.7	2.11	75	628	6.65 ± 0.79
10	11.8	1.03	89	1096	6.01 ± 0.64	20	13.7	2.10	75	628	5.35 ± 0.53
10	12.4	1.00	103	1191	3.54 ± 0.73	10	10.5	2.02	57	504	6.37 ± 1.26
10	12.4	1.00	103	1191	4.31 ± 0.83	10	14.1	2.71	42	501	5.03 ± 1.02
10	18.9	1.53	68	1192	1.80 ± 0.29	10	12.3	2.31	68	514	5.75 ± 0.86
10	19.0	1.53	104	1194	4.92 ± 0.58	10	10.9	1.91	82	547	12.30 ± 1.70
10	12.2	0.99	82	1187	2.41 ± 0.50	10	15.5	2.73	57	547	7.41 ± 1.93
10	10.9	0.89	79	1186	2.01 ± 0.42	10	15.6	2.76	57	547	6.35 ± 1.28
20	13.3	1.07	107	1208	3.41 ± 0.79	10	13.5	2.39	56	548	9.25 ± 1.05
20	13.4	1.07	107	1208	4.00 ± 0.39	10	13.8	2.43	56	548	6.47 ± 0.71
20	13.4	1.07	146	1208	2.73 ± 0.90	10	11.8	2.11	75	539	8.92 ± 1.08
20	20.9	1.67	94	1207	2.25 ± 0.42	10	11.3	1.67	95	652	5.90 ± 1.03
20	20.9	1.68	94	1207	1.29 ± 0.31	10	11.3	1.67	95	652	6.90 ± 0.77
20	12.8	1.02	156	1210	4.16 ± 1.26	20	11.3	1.62	97	673	5.19 ± 0.66
20	12.1	1.26	91	933	1.86 ± 0.49	20	11.3	1.62	97	673	4.57 ± 0.66
20	17.1	1.76	89	938	2.05 ± 0.19	10	17.6	2.61	61	653	7.49 ± 1.11
20	20.9	2.15	73	938	1.29 ± 0.20	10	17.6	2.60	61	653	7.63 ± 1.02
20	21.0	2.16	73	936	1.24 ± 0.39						
10	12.1	1.27	81	920	2.20 ± 0.50	20	14.5	1.21	86	1158	2.20 ± 0.37
10	12.1	1.27	81	920	3.33 ± 0.95	10	16.0	1.29	81	1196	5.91 ± 0.92
10	13.9	1.45	71	923	7.80 ± 1.08	10	26.8	2.26	69	1147	5.93 ± 1.49
10	13.9	1.46	71	923	4.23 ± 0.63	20	11.4	0.93	111	1191	3.97 ± 1.67
10	14.3	1.50	76	920	3.69 ± 0.78	20	11.4	0.93	111	1189	5.38 ± 1.00
10	19.0	1.98	80	925	3.83 ± 1.27	20	9.9	0.80	129	1190	6.35 ± 1.15
10	19.0	1.98	80	925	2.24 ± 0.68	20	9.9	0.80	129	1189	7.09 ± 1.14
10	12.6	1.61	98	760	4.68 ± 0.82	20	12.4	1.37	77	877	1.73 ± 0.41
10	12.6	1.61	98	760	5.80 ± 1.88	20	12.4	1.38	77	869	2.23 ± 0.61
10	11.7	1.50	67	754	6.11 ± 1.05	10	12.4	1.38	77	867	4.63 ± 0.84
10	11.8	1.51	66	754	6.62 ± 0.68	10	15.0	1.63	65	887	6.48 ± 0.68
10	21.1	2.69	59	757	2.64 ± 0.69	10	15.2	1.78	89	824	3.09 ± 1.12
10	21.2	2.70	59	757	3.16 ± 0.82	20	24.1	2.71	58	858	1.26 ± 0.30
20	12.2	1.55	67	759	2.30 ± 0.31	20	16.5	1.81	59	880	1.69 ± 0.18
20	12.2	1.55	67	759	1.82 ± 0.23	20	11.6	1.79	58	628	1.68 ± 0.56
20	17.2	2.16	73	767	2.06 ± 0.24	20	19.0	2.87	54	640	2.59 ± 2.54
20	11.9	1.49	91	770	2.26 ± 0.28	20	19.0	2.88	54	635	2.17 ± 0.48
20	11.9	1.50	91	770	2.64 ± 0.30	10	16.0	2.55	41	604	4.98 ± 1.01
20	25.1	3.15	43	769	0.96 ± 0.14	10	16.0	2.48	42	622	3.83 ± 0.79
20	25.2	3.16	43	769	0.97 ± 0.11	10	19.9	3.05	34	629	2.67 ± 0.71
20	38.6	4.81	33	775	0.67 ± 0.11	10	19.9	3.00	35	641	4.02 ± 0.51
20	38.6	4.80	33	775	0.69 ± 0.08	10	12.5	1.47	69	821	7.26 ± 1.44
20	12.4	1.77	57	675	2.56 ± 0.28	10	12.5	1.46	70	825	8.37 ± 2.10
20	18.9	2.66	59	688	1.83 ± 0.19	20	22.9	2.74	46	810	1.32 ± 0.25
20	18.9	2.66	59	688	1.62 ± 0.30	20	18.1	2.00	51	874	0.93 ± 1.28
20	11.7	1.67	49	676	1.56 ± 0.18	20	18.1	2.02	51	865	1.04 ± 0.19
20	11.7	1.67	49	676	1.31 ± 0.16	20	13.6	1.56	67	861	1.76 ± 0.30
10	13.2	1.95	53	655	5.89 ± 0.60	20	13.8	1.54	67	861	2.45 ± 0.31
10	13.3	1.96	53	655	6.79 ± 1.37	20	16.5	1.89	66	843	1.46 ± 0.28
10	15.7	2.29	69	661	6.44 ± 0.81	20	16.5	1.88	66	845	1.67 ± 0.45
10	15.7	2.29	69	661	7.18 ± 0.78	20	12.2	1.38	90	852	2.78 ± 0.60
10	12.7	2.10	75	585	5.86 ± 1.06	20	12.5	0.95	107	1266	7.08 ± 1.38
10	11.6	1.94	48	579	3.33 ± 0.39	20	12.5	0.95	106	1262	9.18 ± 2.44
10	11.7	1.94	47	579	2.14 ± 0.26	20	20.9	1.62	62	1244	2.12 ± 0.27
10	19.8	3.15	50	606	1.74 ± 0.20	20	13.2	1.02	99	1249	2.65 ± 0.52
10	20.0	3.18	50	606	1.47 ± 0.23	20	15.7	1.23	100	1231	3.40 ± 0.81
20	18.9	1.45	109	1263	1.41 ± 0.30	20	15.7	1.24	100	1228	3.34 ± 0.99
20	18.9	1.45	109	1263	1.22 ± 0.39	10	15.7	1.23	100	1236	9.96 ± 1.90
20	13.4	1.02	91	1268	2.72 ± 0.55	20	18.0	1.46	69	1188	4.61 ± 0.48

^aThe measurements are reported in the sequence in which they were obtained. Those above the space were made in reactor 1, the others in reactor 2.

One hundred eighty-one k_2 measurements were made, of which one hundred forty were considered acceptable. One of the dif-

ficulties encountered was the maintenance of a constant Al flux from the W coil and in turn a constant $[\text{AlO}]_{\text{max}}$. The $[\text{AlO}]_{\text{max}}$

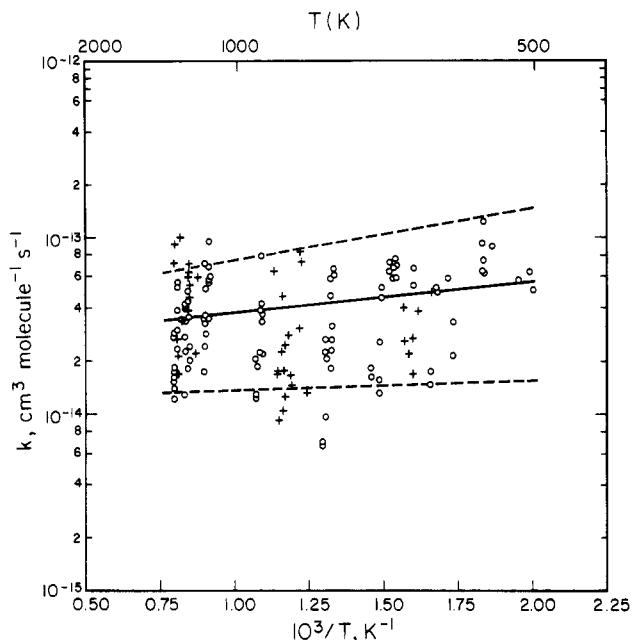


Figure 3. Arrhenius-type plot for the AlO + CO₂ → AlO₂ + CO reaction. Individual data points as measured: (O) reactor 1; (+) reactor 2. (—) Calculated rate expression given in the text. (---) Error limits of the rate expression as discussed in the text.

was recorded at both the beginning and the end of a k_2 measurement. If the difference between these two $[\text{AlO}]_{\text{max}}$ divided by their average exceeded ± 0.50 , the k_2 measurement was discarded. In addition, if the correlation coefficient r of a $\ln [\text{AlO}]_{\text{rel}}$ vs. $[\text{CO}_2]$ plot was less than 0.75 the k_2 measurement was discarded. The second requirement was used to remove values where $[\text{AlO}]_{\text{max}}$ had drifted but returned close to the original value.

The k_2 measurements are summarized in Table I. It may be seen from the data that the k_2 values are independent of $[\bar{M}]$ from 8.0×10^{16} to 4.8×10^{17} cm⁻³, average gas velocity from 30 to 170 m s⁻¹, oxidant inlet position, and the reactor used. It should be noted that the pressures, and hence $[\bar{M}]$, given are averages. When CO₂ was added the pressure increased slightly. The lowest and highest downstream pressures recorded were averaged and corrected^{3,13} to obtain the average pressure in the reaction tube. Temperature measurements were made in the reaction tube from the observation window to the inlet position at 5-cm intervals. These measurements were corrected^{3,13} to obtain actual gas temperatures and then averaged to obtain the given temperatures. The standard deviation about the average temperature varied from ± 6 to ± 48 K depending on the reaction conditions. Such variation is inherent in HTFFR work^{3,13} and is taken into account in the error analysis.

The k_2 data are plotted vs. inverse temperature in Figure 3. Analysis of these data results in

$$\ln [k_2(T)/(\text{cm}^3 \text{ molecule}^{-1} \text{ s}^{-1})] = \ln \{[\exp(-31.31 \pm 0.38) \pm 0.1 \exp(-31.31)]/(\text{cm}^3 \text{ molecule}^{-1} \text{ s}^{-1})\} + (400 \pm 280)/T$$

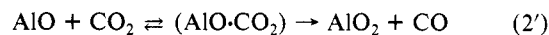
which leads to¹⁴

$$k_2(T) = (2.5 \pm 1.3) \times 10^{-14} \exp[(400 \pm 280)/T] \text{ cm}^3 \text{ molecule}^{-1} \text{ s}^{-1}$$

In these expressions the error limits of the A factor and the exponential are two standard deviations; in addition a 10% systematic error for the uncertainty in the flow profile factor³ has been added to the uncertainty of the A factor.

Reaction 2 shows no evidence of upward curvature, in contrast to reaction 1. This is in accord with the prediction based on the higher ionization potential of AlO compared to Al. The slight

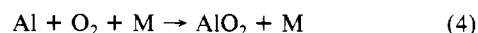
negative activation energy indicated by our data suggests a reaction involving an intermediate complex which preferentially dissociates to the original reactants, the most common cause for zero or negative temperature dependences in bimolecular reactions,² i.e.



The very small preexponential factor also suggests the dominance of the dissociation to the reactants. This behavior is very similar to that observed for reaction 3, for which $k_3(T) = (2.3 \pm 0.6) \times 10^{-13} \exp[(333 \pm 170)/T]$ was obtained.¹⁰ The latter also shows a rather small A factor, though an order of magnitude larger than that for reaction 2.

The absence of a positive activation energy in the AlO/CO₂ reaction indicates a new bond of at least 127 kcal mol⁻¹, thus increasing the apparent disagreement with the 100 ± 9 kcal mol⁻¹ value of Ho and Burns.¹¹ In the HTFFR work on reactions 2 and 3 only the disappearance of AlO is observed. The electronic spectrum of AlO₂ is unknown, but AlO₂ appears the only reasonable product for these pressure-independent reactions. While Ho and Burns directly observed a species of the AlO₂ mass, their mass spectrometer evaporation experiments also cannot elucidate the structure of the product. It would appear likely that the AlO₂ produced in both types of experiments is not identical. Results from Hartree-Fock and MNDO calculations indicate several possible structures for AlO₂, with linear OAIO as the most stable configuration, followed by linear AlOO and cyclic AlO₂, some 22 and 38 kcal mol⁻¹ less stable, respectively.¹⁵ Linear OAIO may also be expected to be the most stable structure by analogy to the well-known linear OBO,¹⁶ which has been identified by LIF as the product of the BO + O₂ reaction.¹⁷ The existence of AlOO with a 100° angle has been demonstrated by infrared absorption spectroscopy in N₂ frozen-matrix studies of reactions of Al atoms with O₂ and O₃.¹⁸ It is thus likely that OAIO is the product of reactions 2 and 3, while AlOO could be that from the Al₂O₃ evaporation experiments. One indication for this hypothesis is that in Ho and Burns work the other triatomic species observed Al₂O was present in concentrations three orders of magnitude higher than AlO₂, while more similar concentrations a priori have been expected. This may imply that OAIO does not form a stable positive ion, which could also be the reason that previous evaporation-mass spectrometer experiments failed to detect AlO₂ unambiguously.

Mann and Weaver have made a mass spectrometric survey of the Al/O₂ reaction system and detected both AlO and AlO₂.¹⁹ However, the pressure dependence of the AlO₂ formation was not established. Hence it could have formed from the abstraction reaction 3, or the addition reaction



The latter is again likely to form AlOO or cyclic AlO₂. The structure of the AlO₂ formed in various experiments thus remains an open question and the published^{8,11} thermochemical values for AlO₂ should be used with caution.

Acknowledgment. Research sponsored by the Air Force Office of Scientific Research, Air Force Systems Command, USAF, under Grant No. AFOSR-82-0073.

Registry No. AlO, 14457-64-8; CO₂, 124-38-9.

(15) Data Sheet on AlO₂ (31 Dec 1979) in ref 8.

(16) Herzberg, G. *Molecular Spectra and Molecular Structure. III. Electronic Spectra and Electronic Structure of Polyatomic Molecules*; Van Nostrand-Reinhold: New York, 1966; p 184 ff.

(17) Llewellyn, I. P.; Fontijn, A.; Clyne, M. A. A. *Chem. Phys. Lett.* **1981**, *84*, 504.

(18) Sonchik, S. M.; Andrews, L.; Carlson, K. D. *J. Phys. Chem.* **1983**, *87*, 2004.

(19) Mann, D. M.; Weaver, D. P., AFRPL Technical Report 84-53, Edwards AFB, CA, August 1984.